Journal of Aerosol Science 79 (2015) 126–139

Contents lists available at ScienceDirect

Journal of Aerosol Science

journal homepage: www.elsevier.com/locate/jaerosci

Monte Carlo modelling of particle resuspension on a flat surface

J.G. Benito [a,*], K.A.Valenzuela Aracena [a], R.O. Uñac [a], A.M. Vidales [a], I. Ippolito [b]

[a] INFAP, CONICET, Departamento de Física, Facultad de Ciencias Físico Matemáticas y Naturales, Universidad Nacional de San Luis, Ejército de los Andes 950, D5700HHW San Luis, Argentina
[b] Grupo de Medios Porosos y CONICET, Facultad de Ingeniería, Universidad de Buenos Aires, Paseo Colón 850, 1063 Buenos Aires, Argentina

ARTICLE INFO

Article history:
Received 10 June 2014
Received in revised form
16 October 2014
Accepted 17 October 2014
Available online 29 October 2014

Keywords:
Resuspension
Monte Carlo simulation
Adhesion
Turbulence

ABSTRACT

A model for the resuspension of a monolayer of particles deposited on a flat surface is developed based on a Monte Carlo simulation of the phenomenon. Particles deposited on the surface are attached to it through an adhesion force. A turbulent flow is assumed to be responsible for the resuspension of particles. The stochastic process used for particle resuspension is based on the evaluation of probabilities depending on the ratio between adhesion and aerodynamic forces and using a Metropolis function. Although simple, the present model accounts for the main features of the resuspension flux observed experimentally and by other models. The model is able to clearly show the role that the parameters of the force distributions (both adhesion and turbulent) have on the short- and long-term resuspension flux, and it captures the intrinsic stochastic nature of the resuspension process.

1. Introduction

The problem of resuspension of already deposited fine particles on a surface has a long history, and has captured the attention of researchers since many decades. Its presence in a wide set of industrial and environmental scenarios makes its study and description an important chapter in aerosol science (Bowling, 1988). In particular, one of the main concerns has been to obtain perfectly clean surfaces for micro and nanoelectronic technology. In addition, there is the problem of the release of radioactive particles to the environment during nuclear accidents (Reeks et al., 1988; Zhang et al., 2013; Stempniewicz et al., 2008).

Furthermore, the problem of the resuspension not only concerns the above domains, but also causes serious difficulties in mining production. Indeed, mining operations are notable in the amount of generated particulates, the extent of polluted areas and toxicity, when compared with other sources of dust and aerosol emissions (Csavina et al., 2012; Stovern et al., 2014).

However, many aspects of the problem still remain as an open question for researchers. The complexity of the problem is based on the difficulties in the measurement of the microscopic adhesion forces that result from the particles–surface interaction through a blend of mechanical stress, chemical bonds and physical attractions. For example, knowledge of the particle size and the surface roughness is crucial for the calculation of the reduction and spread in the adhesion force.

* Corresponding author.
E-mail address: jbenito@unsl.edu.ar (J.G. Benito).

http://dx.doi.org/10.1016/j.jaerosci.2014.10.006
0021-8502/

However, given the serious experimental difficulties in their determination, a theoretical approach to this description is required to model particle–surface interactions. Other difficulties are the different flow conditions and the respective aerodynamic forces involved.

Besides, in practice, many problems of particle resuspension involve the presence of multilayer deposits, which add greater complexity related to mutual obstruction of particles, the formation and eventual resuspension of clusters and the dependence of the resuspension process on the structure of the deposit (Ziskind, 2006; Gradón, 2009; Boor et al., 2013; Henry & Minier, 2014b; Hanus et al., 2007). Many models have been developed in the last two decades. Comprehensive reviews concerning resuspension models can be found in Zhang (2011), Ziskind et al. (1995), Henry & Minier (2014a) and Stempniewicz et al. (2008). In general, theoretical models developed to simulate and predict the resuspension properties are divided into two categories: those based on the balance resulting from the aerodynamic and adhesive forces acting on a particle, called quasi-static models (Reeks & Hall, 2001); and those based on the removing of particles by energy accumulation, described in terms of the accumulation of kinetic energy of the flow, called dynamic models. However, given the large amount of diverse work, the debating points and the models that may not fit in these two raw categories, a new classification has been recently proposed to account for recent developments in resuspension models (Henry & Minier, 2014a).

In most cases, the models reproduce the experimental behavior, characterized by an initial or short-term resuspension, and by a long-term resuspension described by a $1/t$ decay. In general, the condition for the particles to resuspend is that the aerodynamic forces have to be greater than the forces of adhesion. In particular, we want to highlight the kinetic model of Wen & Kasper (1989), based on the analogy between the process of resuspension supported by the balance of forces, and the kinetics of the first order reaction that describes the desorption of molecules from a heterogeneous surface, with a constant resuspension rate. Many models are based on a balance of forces that involves the possibility of instantaneous resuspension of particles when the removal forces are greater than the adhesion forces. Nevertheless, other models allow the movement of the particle on the surface before reentrainment (Guingo & Minier, 2008; Henry et al., 2012; Henry & Minier, 2014b; Fu et al., 2013).

Given the fact that the resuspension phenomenon can be treated as a stochastic process, this paper proposes a model based on a Monte Carlo (MC) simulation. Our aim is to use an algorithm that takes into account the analogy between the release process of particles and first order chemical reactions. With the help of the phenomenological Arrhenius expression for the determination of the resuspension rate, we show that the Metropolis function (Binder & Heermann, 1992), used as the transition probability between configuration states, is able to describe the main features of the resuspended particle flux for the case of a monolayer of particles deposited onto a flat surface and subjected to a turbulent flow. In this case, there will be a process activated by removal forces, as for the case of the kinetic model of Wen & Kasper (1989), instead of being activated by the surface temperature. We consider that the resuspension rate depends on the ratio between the adhesive force and the removal force acting on a particle (Zhang, 2011). We should clarify here that other MC models (Goldasteh et al., 2013; Fu et al., 2013) use the balance between moments of adhesion and hydrodynamic forces. As one can expect, the choice of a force balance or a moment balance approach is related to the assumed motion of particles: rolling, described by moment balance, while sliding and lifting are properly described by a force balance (Ibrahim et al., 2008). As emphasized in a recent review (Henry & Minier, 2014a), the relative importance of rolling and 'burst-type' resuspension (by turbulent flows) depends on the size of particles: small particles which are well embedded in the viscous sublayer are more sensitive to rolling motion while larger particles are more affected by 'burst-type' resuspension.

The main difference between our present model and the models before is that we employ a MC method to deal with resuspension kinetics. As will be explained below, in the present model, the probability of a particle to be released from the surface is not necessary equal to one if the adhesion force is less than the aerodynamic force and, moreover, the probability is not equal to zero if the aerodynamic force is less than the adhesion force. As it will be seen, this model allows recovering the main aspects of the resuspension process. Thus, the novelty here is the inclusion, through a MC method, of the stochastic nature of the removal forces due to the flow and the adhesion forces between particles and the surface.

In the following section, the description of the model and a brief explanation of the Monte Carlo method, are presented. In addition, the type of distribution assumed for aerodynamic and adhesion forces is also presented, along with the rules of the stochastic process applied in the simulation routine. The complete set of the simulation results is displayed in Section 3, which is divided into four subsections that present simulations for monodisperse adhesive forces, rough surfaces, a phase diagram and a final comparison with experimental data for fractional mass resuspension vs. time. Section 4 presents a detailed discussion of all the obtained results and, finally, the conclusions are presented in Section 5.

2. Model description

The model proposed here, as the one of Wen & Kasper (1989), describes the resuspension of particles from a surface as a first order chemical reaction, such as the desorption process from a heterogeneous surface (Zhdanov, 1991). For the expression of the rate constant, empirical or phenomenological equations are used. One of the most used is the Arrhenius Law (Moelwyn Hughes, 1971). In this case, the rate constant k is given as $k(F)=A\exp(-F)$, where A, the preexponential factor, and F, the relative balance between the adhesion force and the removing force in the process, are the apparent Arrhenius parameters.

In the model of Wen & Kasper (1989), the rate equation is integrated assuming a particular distribution for F (uniform), giving analytical solutions for the concentration of particles on the surface and the gas stream, as a function of time.

In the last decades, MC methods have demonstrated to be a versatile and powerful tool to address molecular processes on surfaces (Binder & Heermann, 1992). We propose here an extension of this tool, to describe the kinetic mechanisms governing the resuspension of particles from a surface.

2.1. Brief description of the Monte Carlo method

It is very well known that statistical mechanics in the Canonical ensemble allows to find the mean value of any macroscopic quantity, A_α, which depends on the state α but, it has the drawback that the partition function of the whole system has to be calculated, which is not an easy job (Binder & Heermann, 1992).

The underlying idea of the MC simulation is to replace the calculation of the average of a variable by using an approximation of it over a chain of states that are chosen stochastically, following the equilibrium probability distribution of states. Thus, the main idea is to numerically simulate the temporal evolution of the system under study through that chain of states.

Metropolis et al. (1953) demonstrated that starting from any arbitrary initial state and using any transition probability fulfilling the so-called *detailed balance*, the chain of generated states tends to be the equilibrium state distribution after a sufficiently large number of transition attempts. The transition probability used by Metropolis is often referred as Metropolis function (Binder & Heermann, 1992).

For the case of non-equilibrium systems, as the one studied in the present paper, we have to take into account the temporal evolution of the transition probabilities in the system (Binder & Heermann, 1992). Thus, in order to study the temporal evolution of a simulated process, it is essential to know the relationship between the actual time spent in the process and the number of MC steps (MCS). This correlation is often known as Kinetic Monte Carlo simulation. When the transitions are carried out in equal time intervals, Δt, the actual elapsed time after N_s steps is simply $t = N_s \Delta t$. However, this is not that easy in most cases.

Consider a single-particle process on a surface represented by a lattice of sites. A particle at state i can make a transition to different states j, with transition velocities w_{ij}, but, for the present model, we just consider one possible type of transition, i.e., a deposited particle can resuspend to the gas stream. However, other possible final states could be considered, depending on the degree of complexity added to the model and the features wanted to be taken into account. Thus, let $r_i = w_{ij}$ be the transition rate for a particle at state i to the new final state j, and $R = \Sigma_{i=1}^{N} r_i$ the total transition rate for the whole system of N particles.

Now we wonder what is the probability of the system to perform a transition during the interval $(t,\ t+dt)$. This probability, $P(t)\ dt$, is given by (Poisson Process) (Sales et al., 1996)

$$P(t)dt = \mathrm{Re}^{-Rt}\ dt \tag{1}$$

Eq. (1) is the time probability distribution for a transition.

In MC simulations, the variable t, which is distributed following $P(t)\ dt$, is replaced by a random number ξ, uniformly distributed in the interval (0,1) (Sales et al., 1996). Thus, it is necessary that $P(t)\ dt$ be equal to $d\xi$, giving

$$t = -\frac{\ln(\xi)}{R} \tag{2}$$

Namely, if we take a random number ξ uniformly distributed in (0,1), Eq. (2) gives the actual time in which the system performs a transition. Thus, the total transition rate R (which is known in the simulation) along with Eq. (2), determine the relationship between the "virtual" MC time and the "actual" time of the system. It should be mentioned that in the present Metropolis algorithm there is no correlation between the state chosen at time t and the one chosen at time $t+\Delta t$.

This MC method has been extensively used to study the kinetics of molecular processes on surfaces (Binder & Heermann, 1992; Meng & Weinberg, 1994; Sales & Zgrablich, 1987; Sitja et al., 2010). For example, Sales & Zgrablich (1987) have used a MC simulation to analyze joint effects of heterogeneity and adsorbate–adsorbate interactions. They first treated the case of two (or more) type of sites, with fixed adsorptive energies and arranged in different structures on a linear chain, and then generalized to two-dimensional lattices with a Gaussian energy distribution for each type of site.

2.2. Resuspension model and forces involved

Keeping in mind the method described above, we consider an idealized lattice structure of a monolayer deposit of $N_0 = 10{,}000$ monosized particles with radius $R_p = 0.59 \times 10^{-6}$ m, typical of aerosol samples. The distance between particles is not relevant in the present model since they do not interact with each other. Proofs were made to check if the results are dependent on the number of particles. We find that a monolayer of 10,000 particles behaves the same as one of 30,000 particles.

Once the particles are defined, an adhesion force, F_a, sampled from a lognormal distribution, is assigned to each of them. Although non lognormal distributions can also occur (Zhou et al., 2003), the choice of this kind of distribution is based on longstanding experimental evidence indicating a lognormal distribution for adhesive forces (Bohme et al., 1962; Reeks et al.,

1988; Matsusaka et al., 1991; Taheri & Bragg, 1992; Reeks & Hall, 2001; Salazar-Banda et al., 2007; Zhang et al., 2013); its form is given by

$$A(F_a) = \frac{1}{\sqrt{2\pi} F_a \ln \sigma_a} \exp\left[-\frac{1}{2}\left(\frac{\ln(F_a/\mu_a)}{\ln \sigma_a} \right)^2 \right] \tag{3}$$

where μ_a and σ_a are the mean and the dispersion, respectively. As a starting point we take the basic assumptions made by Friess & Yadigaroglu (2001), that the adhesion force between a particle and a flat surface is proportional to the particle radius, i.e., $\mu_a = 2c_a R_p$, where c_a is the constant of adhesion. Both c_a and σ_a are used as variable parameters to test the capacity of the model for predicting different behaviors. In the case of σ_a, we do not try to identify it with experimental values.

The resuspension of a particle is assumed to be caused by a stochastic process resulting from the balance between adhesion forces and the forces exerted by a flow with eventual turbulent bursts, F_b. These aerodynamic forces are assumed to obey a Gaussian distribution as

$$B(F_b) = \frac{1}{\sqrt{2\pi}\sigma_b} \exp\left[-\frac{1}{2}\left(\frac{F_b - \mu_b}{\sigma_b} \right)^2 \right] \tag{4}$$

where μ_b and σ_b are the mean and the dispersion, respectively. The values of these two parameters are varied in order to study their influence on the resuspension process. Here again, we follow the assumptions made by Friess & Yadigaroglu (2001), that $\mu_b = 4c_b R_p^2 \tau_m$, where c_b is the burst constant (here equal to 1) and τ_m is the shear stress. In most cases, we set $\sigma_b = 0.33\mu_b$, which reasonably represents the range of experimental values reported in the literature (Friess & Yadigaroglu, 2001). Nevertheless, we also try values for σ_b totally uncorrelated from μ_b to test the model capability. The different values used for the simulations will be presented in the next section.

Following the Metropolis' scheme explained above, we consider the resuspension of the particles deposited on the flat surface as a single process activated by the turbulent flow. The particles are not allowed to move over the surface neither to be redeposited. In such a case, we can consider a unique resuspension rate r_i for a particle located at site i. We do not apply a relaxation process to keep the equilibrium distribution of particles.

Thus, we can define r_i as

$$r_i = \nu e^{-[(F_a^i - F_b^i)/F_b^i]} \tag{5}$$

where ν is the frequency factor, which, as in other models, is related to the burst frequency.

Eq. (5) represents the expression for the transition rate for an Arrhenius type process, activated by a hydrodynamic force. This corresponds to a first order kinetic process and for that reason the exponent of the exponential is equal to one.

The different steps of the algorithm are as follows (Sales et al., 1996):

(i) Let $r \geq \max\{r_i\}$; $R = N_a r$; $t = t_0$, where N_a is the number of particles still on the surface.
(ii) Obtain a random number ξ; $\Delta t = -\ln(\xi)/R$; $t = t + \Delta t$.
(iii) Select randomly a deposited particle "i".
(iv) Choose randomly an aerodynamic force from the distribution given by Eq. (4).
(v) Evaluate r_i using Eq. (5).
(vi) Obtain a new random number ξ; if $\xi < r_i/r$, then accept the resuspension step at time t.
(vii) Repeat from steps (ii) to (vi) until all the particles resuspend or a certain period of time has elapsed.

It should be said that the $\max\{r_i\}$ is calculated taking into account the extreme cases for both distributions of forces (adhesion and hydrodynamic). The initial state corresponds to N_0 particles deposited on the surface with a given adhesion force to each of them. From this initial configuration, the algorithm starts up by point (i), until all the particles are eventually resuspended.

The algorithm above allows recording the number of particles resuspended as a function of time. We will define the fractional resuspension rate F as

$$F(t) = -\frac{1}{N_0}\frac{d}{dt}N(t) \tag{6}$$

where $N(t)$ is the number of remaining particles per unit of wall surface after resuspension time t. Given that the particles are considered identical, mass flux or particle flux is just a matter of a mass factor.

The time elapsed in one resuspension experiment strongly depends on the chosen parameters, going from 10 min to several days on a CPU with an AMD Phenom II.

3. Results

3.1. Evaluation for the simple case of monodisperse adhesive forces

The first preliminary test of the model corresponds to the simplest case of a monolayer of particles that resuspend from identical adhesive sites (smooth surface). In this case, adhesion forces are all equal, and a value of $F_a = 3.68 \times 10^{-12}$ N is considered here, according to a radius of 0.59×10^{-6} m and parameters taken from Friess & Yadigaroglu (2002). This value corresponds to the adhesion between a smooth surface and a sphere. The aerodynamic forces follow a distribution like that in Eq. (4), with $\mu_b = 6.96 \times 10^{-12}$ N and $\sigma_b = 2.29 \times 10^{-12}$ N, where $\sigma_b = 0.33\mu_b$. This last assumption is based on a reasonable representation of the range of experimental values reported for the dispersion of aerodynamic forces (Friess & Yadigaroglu, 2001, 2002). To express the time in seconds, we choose $\nu = 1\ s^{-1}$ in Eq. (5).

As is well known (Reeks et al., 1988), it is expected that the fraction of resuspended particles will decay exponentially with time. In Fig. 1 we show the results obtained for the fractional flow of particles F vs. time, for a MC simulation with the parameters indicated above. It is worth mentioning that the results in Fig. 1 correspond to the whole resuspension process, until the surface is free of particles. The flux F is calculated as the number of resuspended particles per unit time, divided by the initial number of particles on the surface.

The inset of Fig. 1 shows a semi-log plot to evidence the exponential decay expected for F in the case of monodisperse adhesive forces (Reeks et al., 1988). Moreover, the log–log plot resembles the reentrainment particle concentration found by Wen & Kasper (1989) for the case of a narrow adhesion force distribution. Just to compare, we plot in the figure the line corresponding to the $1/t$ behavior expected for rough surfaces.

3.2. Resuspension from rough surfaces: log-normal distribution of adhesion forces

It is well known that the presence of surface roughness reduces and spreads the adhesive forces on the particles. The spread of the distribution of forces is a consequence of a spread in the surface roughness, and therefore, it is expected that this distribution will be crucial in the resuspension behavior of particles (Reeks et al., 1988).

In our study, we vary the dispersion and the mean of both the adhesion and aerodynamic force distributions according to the values displayed in Table 1. As explained in Section 2, the distribution of adhesion forces is represented through Eq. (3). The values for μ_a are varied by changing c_a while keeping constant the value for the particle radii. We vary σ_a from 1 to 5, which is in the range used in models by other authors (Friess & Yadigaroglu, 2001). For the aerodynamic distribution, we choose values for μ_b in a wide range interval, and also vary σ_b to represent different wind scenarios.

It is worth mentioning that Table 1 represents a non-exhaustive list of all the cases studied in the present work, showing the most representative ones. A set of 25 cases are shown with their corresponding adhesion and aerodynamic force parameters. In addition, a column indicating the overlapping area, Ω, between the two normalized force distributions is provided along with the values for the difference $\Delta\mu = \mu_b - \mu_a$ between the mean values of forces. Finally, the slope resulting from the linear fit of the last points in the resuspension flux vs. time curves is displayed and, in the last column, a reference to the type of behavior found for the flux is given. The nomenclature used in the last column will be explained below.

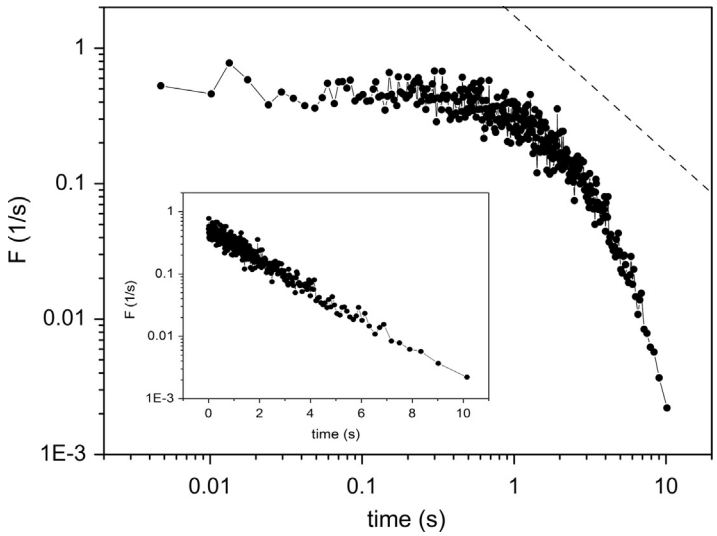

Fig. 1. Resuspension rate from identical adhesive sites. The dashed line indicates the $1/t$ behavior expected for rough surfaces. The inset is a semi-log plot to evidence the exponential decay.

Table 1
Simulation parameters for the most representative studied cases.

Case	*Adhesion force* (N)		*Burst force* (N)		Ω (%)	$\Delta\mu$ (N)	Slope	State region
	μ_a	σ_a	μ_b	σ_b				
1	3.68E−12	1.0	6.96E−12	2.29E−12	54.9806	3.282E−12	−1.35	ST
2	3.68E−13	1.0	6.96E−12	2.29E−12	5.8275	6.593E−12	−3.00	ST
3	3.68E−11	1.0	6.96E−12	2.29E−12	15.6250	−2.984E−11	−1.15	LT
4	3.68E−12	3.5	6.96E−12	2.29E−12	23.4386	3.282E−12	−1.06	LTS
5	3.68E−13	3.5	6.96E−12	2.29E−12	18.3022	6.593E−12	−1.07	LTS
6	3.68E−11	3.5	6.96E−12	2.29E−12	21.1700	−2.984E−11	−1.08	LTS
7	3.68E−12	4.0	6.96E−12	2.29E−12	21.0814	3.282E−12	−1.08	LTS
8	3.68E−12	5.0	6.96E−12	2.29E−12	17.6252	3.282E−12	−1.10	LTS
9	3.68E−12	1.0	6.96E−11	2.29E−11	5.8275	6.593E−11	−3.70	ST
10	3.68E−12	1.0	6.96E−13	2.29E−13	15.6249	−2.984E−12	−1.16	LT
11	3.68E−12	3.5	6.96E−11	2.29E−11	18.3022	6.593E−11	−1.04	LTS
12	3.68E−12	3.5	6.96E−13	2.29E−13	21.1716	−2.984E−12	−1.01	LTS
13	3.68E−12	1.0	6.96E−11	2.29E−13	0.0139	6.593E−11	−4.10	ST
14	3.68E−12	1.0	6.96E−13	2.29E−11	54.3804	−2.984E−12	−2.50	ST
15	3.68E−12	3.5	6.96E−11	2.29E−13	0.1917	6.593E−12	−1.05	LTS
16	3.68E−12	3.5	6.96E−13	2.29E−11	50.1406	−2.984E-12	−1.05	LTS
17	3.68E−12	1.0	6.96E−11	3.43E−11	10.9871	6.593E−11	−3.70	ST
18	2.96E−11	1.0	6.96E−11	2.29E−11	48.2783	4E−11	−1.57	ST
19	2.96E−11	1.5	6.96E−11	2.29E−11	41.5128	4E−11	−1.12	LTS
20	2.96E−11	2.5	6.96E−11	2.29E−11	29.8791	4E−11	−1.11	LTS
21	3.68E−13	1.5	6.96E−12	2.29E−12	12.6858	6.593E−12	−2.04	ST
22	3.68E−11	1.5	6.96E−12	2.29E−12	25.9832	−2.984E−11	−1.08	LT
23	3.68E−13	2.5	6.96E−12	2.29E−12	18.7845	6.593E−12	−1.07	LTS
24	3.68E−11	2.5	6.96E−12	2.29E−12	24.3066	−2.984E−11	−1.24	LT
25	3.68E−11	2.5	6.96E−13	2.29E−13	9.5248	−3.610E−11	−1.12	LT

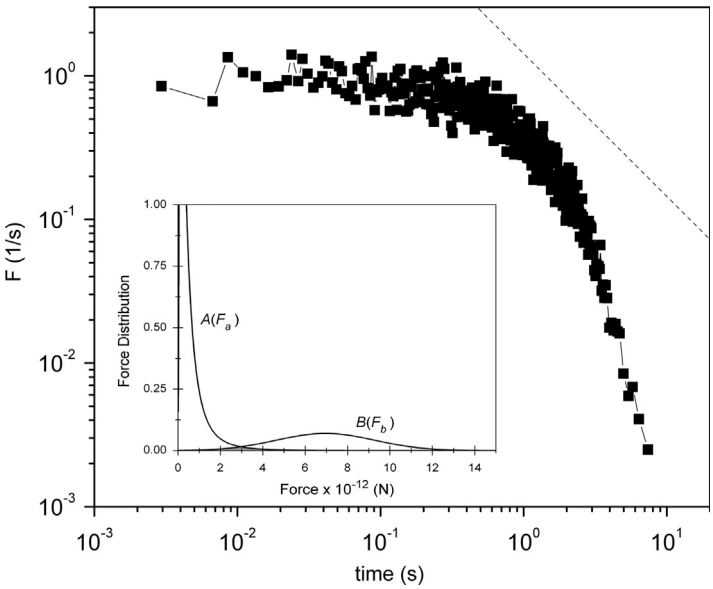

Fig. 2. Flux of resuspended particles as a function of time until the surface is finally free of particles for parameters of case 2 in Table 1. The inset depicts the aerodynamic and adhesion force distributions employed in this simulation, and the overlapping area is shaded.

When comparing the different behaviors according to the values chosen for the aerodynamic and adhesion force parameters, we distinguish three types of cases. The first case is displayed in Fig. 2, where the flux of resuspended particles, F, is shown as a function of time until the surface is finally free of particles. The inset depicts the aerodynamic and adhesion distributions employed in this simulation. The values for the two means and dispersions correspond to case 2 in Table 1. The resuspension rate in Fig. 2 rapidly decreases with time after approximately 1 second. This behavior resembles the one observed for monodisperse adhesive forces (Fig. 1). If we fit the "long-term" part of the curve, we find a slope of −3.00, which is considerably different from the $1/t$ behavior. We mainly relate this fast resuspension to the presence of a large

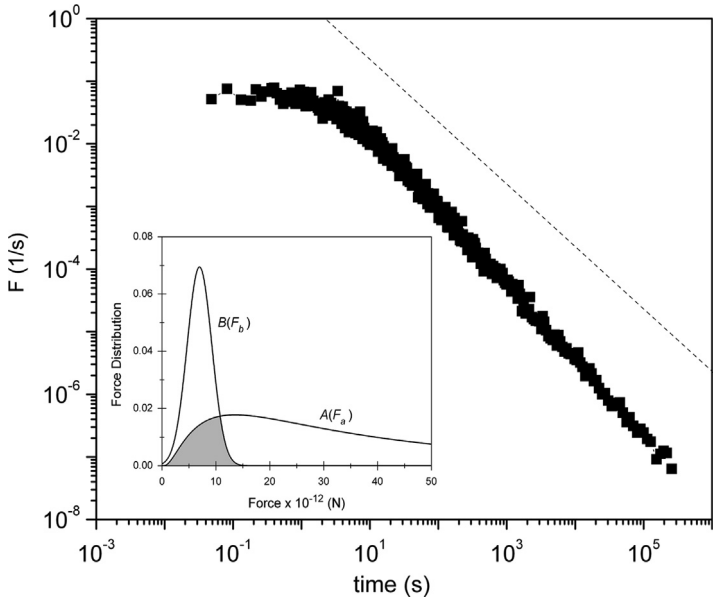

Fig. 3. Flux of resuspended particles as a function of time until the surface is finally free of particles for parameters of case 3 in Table 1. The inset depicts the aerodynamic and adhesion force distributions employed in this simulation, and the overlapping area is shaded.

number of small adhesion forces and a great number of large aerodynamic forces. Moreover, this feature could be associated with the small overlapping area between the two force distributions.

Figure 3 shows the results for F corresponding to the parameters of case 3 in Table 1. Here again, the inset displays the force distributions corresponding to the same aerodynamic force distribution as in Fig. 2 and a two order of magnitude stronger adhesion force. It is clear from the figure that resuspension is strongly delayed with respect to the previous case. The time it takes to achieve full resuspension of the particles is several orders of magnitude greater than before.

This slow resuspension regime is explained by considering the strong increment in adhesion forces, while keeping constant the aerodynamic forces. Note also that the dispersion in adhesion is the same as in the preceding case. The linear fit of the long-term part yields a slope of -1.15, closer to $1/t$ behavior. The overlapping area between curves is greater than in Fig. 2 but, even more important, the mean adhesion force is greater than the mean for turbulent action.

The change in behavior when comparing from Figs. 2 to 3 is linked with the overlap between force distributions, Ω, as well as with the tail of the adhesion force distribution. Thus, we see that short-term resuspension is due to particles encountering higher aerodynamic forces than adhesion forces (related to Ω and to part of adhesion force distribution being lower than the smallest aerodynamic force) while the long-term resuspension is linked to the amount of particles encountering adhesion forces higher than the aerodynamic forces (i.e., part of Ω and part of adhesion force distribution remaining above the highest aerodynamic force). In summary, one could expect that the change in behavior is related to both dispersions in adhesion and aerodynamic forces, as we will see later.

The third type of behavior found is depicted in Fig. 4, according to parameters of case 5 in Table 1. As shown in the inset, the aerodynamic distribution is the same as in Figs. 2 and 3. The mean adhesion force is the same as in Fig. 2, but the spreading is greater. The overlapping area between the distributions is greater than the one in case 2, and of the same order as in case 3. In this case, results for flux vs. time show the presence of a shoulder, indicating some sort of change in regime. The shape of the curve is the typical theoretical result reported by other authors using different models (Friess & Yadigaroglu, 2001; Reeks et al., 1988). In the context of our results, this behavior could be understood as being in between a fast and a slow resuspension regime. We will discuss this feature in the next section. The time elapsed up to full resuspension of the particles, although still quite larger than that corresponding to Fig. 2, is lower here than for Fig. 3. The linear fit of the long-term part yields a slope of -1.07.

According to the values listed in Table 1, we proceed testing the model by systematically changing the different parameters. Figures 5–7 show a set of results corresponding to the three types depicted above.

In Fig. 5, we show three examples for the short-time resuspension case. As indicated in Table 1, the adhesion force distribution is the same for the three curves, and the aerodynamic forces only differ in the dispersion σ_b. The results are quite similar for the three examples, even when σ_b is two orders of magnitude different (cases 9 and 17 against case 13). The overlapping area between the two force distributions is quite small in all cases. Note that the difference between the means μ_b and μ_a, (i.e., $\Delta\mu=\mu_b-\mu_a$,) is the same for all the results. The parameter $\Delta\mu$ will be crucial in determining the occurrence of a short-time resuspension, as we will see below. The dashed line indicates the $1/t$ behavior.

Figure 6 shows three examples for the long time resuspension behavior. The curves for the three cases (indicated in the figure) are quite similar to each other; nevertheless, we can distinguish some features. The three initial values for the flux

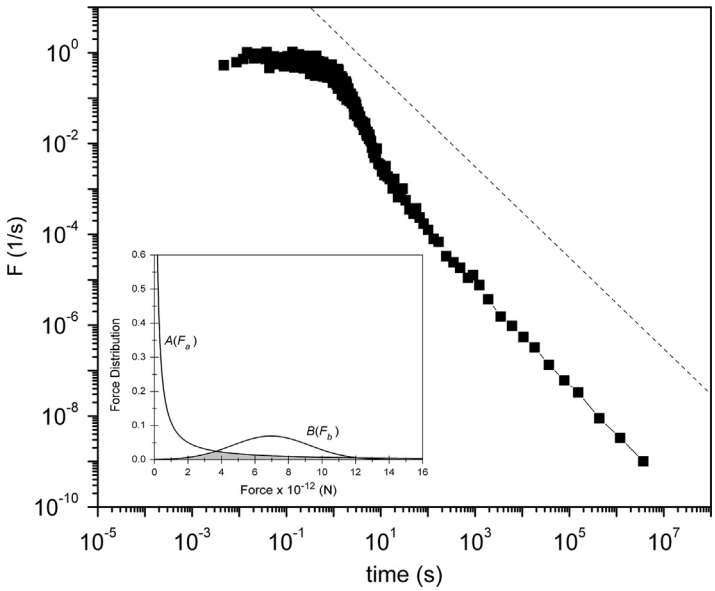

Fig. 4. Flux of resuspended particles as a function of time until the surface is finally free of particles for parameters of case 5 in Table 1. The inset depicts the aerodynamic and adhesion force distributions employed in this simulation and the overlapping area is shaded.

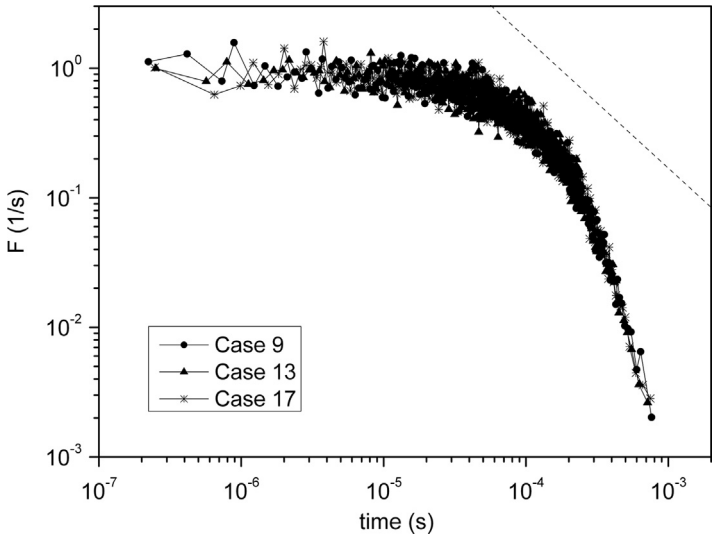

Fig. 5. Set of curves for short-time resuspension. Parameters correspond to cases 9, 13 and 17 in Table 1. Note that the behavior is similar for the three cases.

are slightly different. For case 22, the flux is greater because μ_b is larger, so is σ_b. On the other hand, the smaller flux is found in case 25, where the flow parameters are the same as in case 10, but the adhesion forces are one order of magnitude greater. Note that a lower flux corresponds to a lower value for Ω.

Figure 7 corresponds to cases 4, 11 and 15 in Table 1, where the two regimes, short- and long-term resuspension, are clearly observed. Here again, the dashed line indicates the $1/t$ behavior expected for long-term resuspension.

Looking at the values in Table 1, we observe that the decisive factor in changing behavior with respect to the results in Fig. 5, is the increase in the dispersion of the adhesion forces. On the other hand, despite that the values of the flow forces change in each case, the results shown in Fig. 7 are very similar to each other; nevertheless, we can distinguish some interesting features. The initial value of the flux is slightly different in each example, and the three curves intersect at approximately 4.7 s to invert their relative positions in the long-term resuspension region (see the inset). This behavior is correlated with the overlapping degree between force distributions. As soon as $\Delta\mu > 0$, the short-term resuspension flux is slightly greater for smaller Ω. This means that a low value of Ω is ensuring a greater likelihood for particle reentrainment. Moreover, when $\Delta\mu < 0$, our simulations indicate that the trend is the opposite, that is, the short-term resuspension flux slightly increases with decreasing Ω. Here again, the presence of a low degree of overlap between the adhesion force

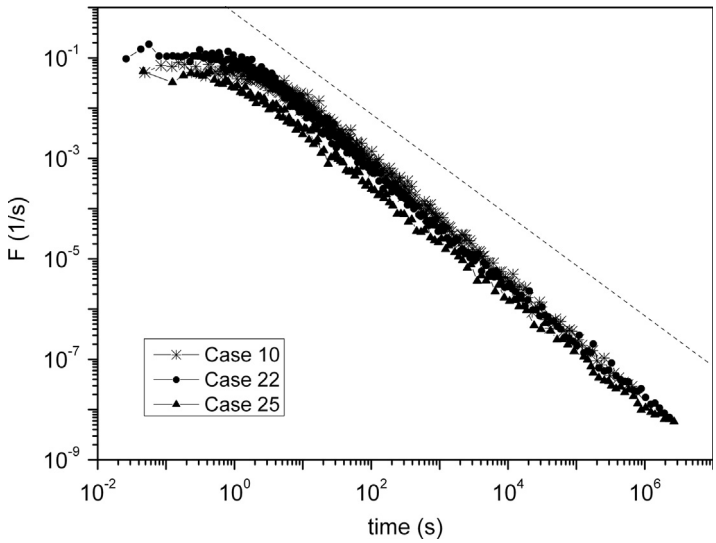

Fig. 6. Set of curves for long-time resuspension without shoulder. Parameters correspond to cases 10, 22 and 25 in Table 1.

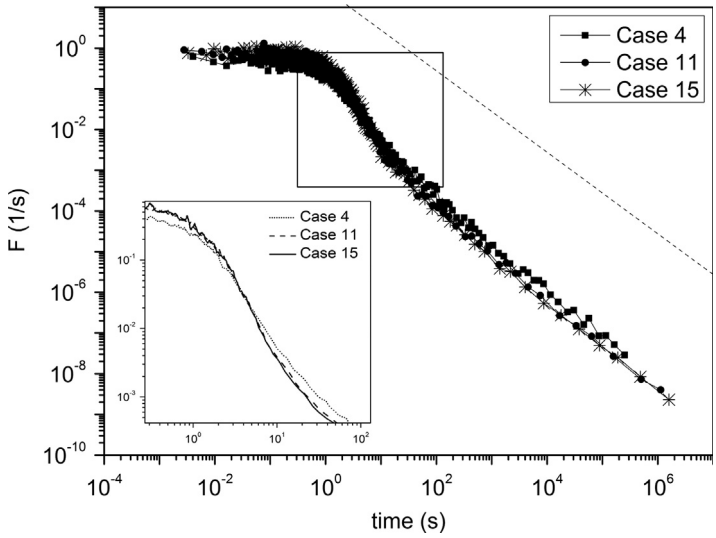

Fig. 7. Three examples of resuspension curves presenting shoulders. Parameters correspond to cases 4, 11 and 15 in Table 1. The inset is a zoom of the curves around $t=4.7$ seconds when they intersect to invert their relative positions in the long-term resuspension region.

distribution and the aerodynamic force distribution, whose mean is lower than the mean for adhesion, lowers the chance of particles for being resuspended. Nevertheless, it is worth noting that there must be a great change in Ω to produce a slight effect in the resuspension curves.

3.3. Phase-diagram for resuspension behavior

From the results shown so far, the following question arises: which are the main parameters characterizing the different resuspension behaviors? To answer this question, we build two phase diagrams with the complete set of numerical simulations explored.

The first one is displayed in Fig. 8, where the axes represent the range of values used for $\Delta\mu$ and σ_a. The lines delineate the three regions with different behavior. They are a guide to the eye and are drawn just to isolate the three regions. Filled circles represent the cases where resuspension takes a long time and the curve does not present a shoulder (as in Fig. 6). Open circles represent the cases with shoulder (as in Fig. 7), and asterisks indicate the short time resuspension runs. We name the three regions as LT, LTS and ST, respectively. The numbers indicate the label of the corresponding simulation run. There are a total of 36 runs displayed in the diagram. As seen, some points are overlapped because they correspond to runs with the same couple of parameters ($\Delta\mu$, σ_a) but different Ω. All such overlapped cases belong to the same type of behavior

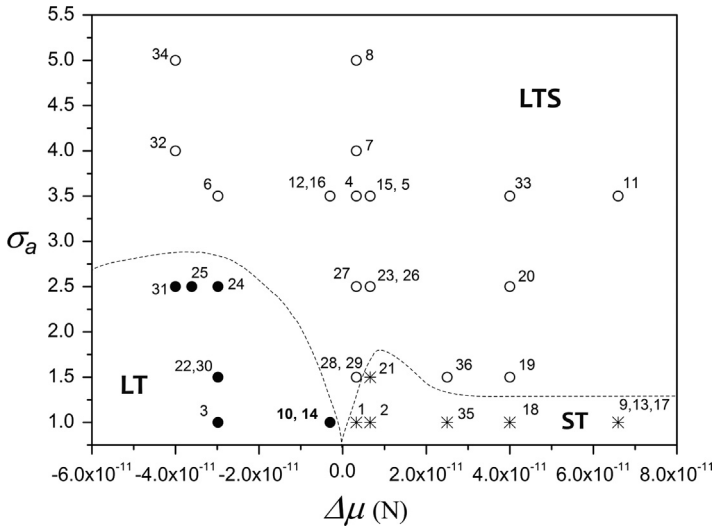

Fig. 8. Phase-diagram for all the 36 cases studied, and using σ_a and $\Delta\mu$ to span the different phases. The dashed lines and the letters indicate the different phase regions. They are just a guide to the eye. The numbers indicate the simulation runs. The numbers in bold correspond to the only two cases where the region of belonging is different.

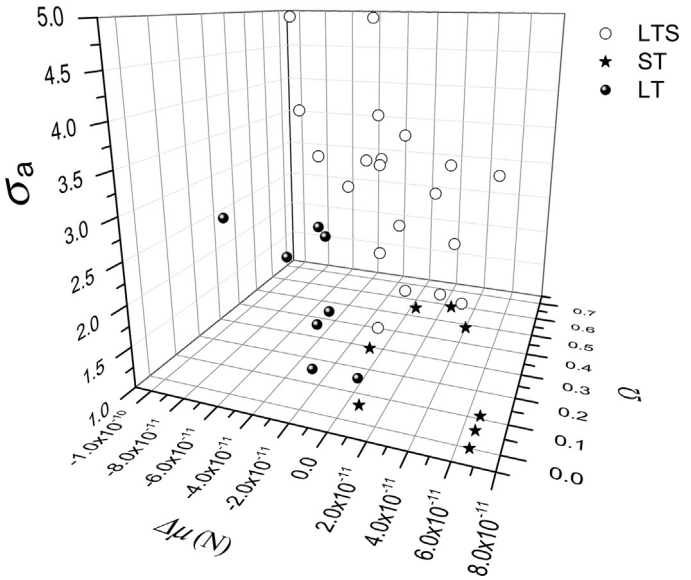

Fig. 9. Three dimensional phase-diagram where Ω is added to the set of parameters in Fig. 8. Filled circles belong to the LT region; open circles belong to cases with shoulder, and stars indicate the short time resuspension runs.

(for instance 9, 13 and 17 are all ST cases), except cases 10 and 14 that differ in their behavior: case 10 belongs to an LT phase (as seen in the figure) and case 14 to an ST phase (not shown in the figure). The numbers of these cases are in bold in the figure.

The two selected parameters are able to distinguish quite well the three cases found in the simulations. The LT region only takes place for $\Delta\mu < 0$ and small to medium values for σ_a. The ST phase is achieved mostly for small σ_a and $\Delta\mu > 0$. There is an exception for case 14, where the low value for Ω makes the difference and modifies the expected behavior. Finally, the LTS region is the largest one for the range of parameters employed and it is bounded by the other two. It is observed that for sufficiently large dispersion in the adhesion forces, a shoulder is expected regardless of the value of $\Delta\mu$. For small σ_a, the analysis is not that simple and the value of Ω starts to play a role.

Complementing the description above, we present in Fig. 9 the same three-phase-diagram, but in a 3D version where the parameter Ω is now included. Here, the regions of different behavior are not so clearly separated. Nevertheless, we observe that the ST region is confined to the base of the diagram, the LT region is to the down-left corner, and the more spread

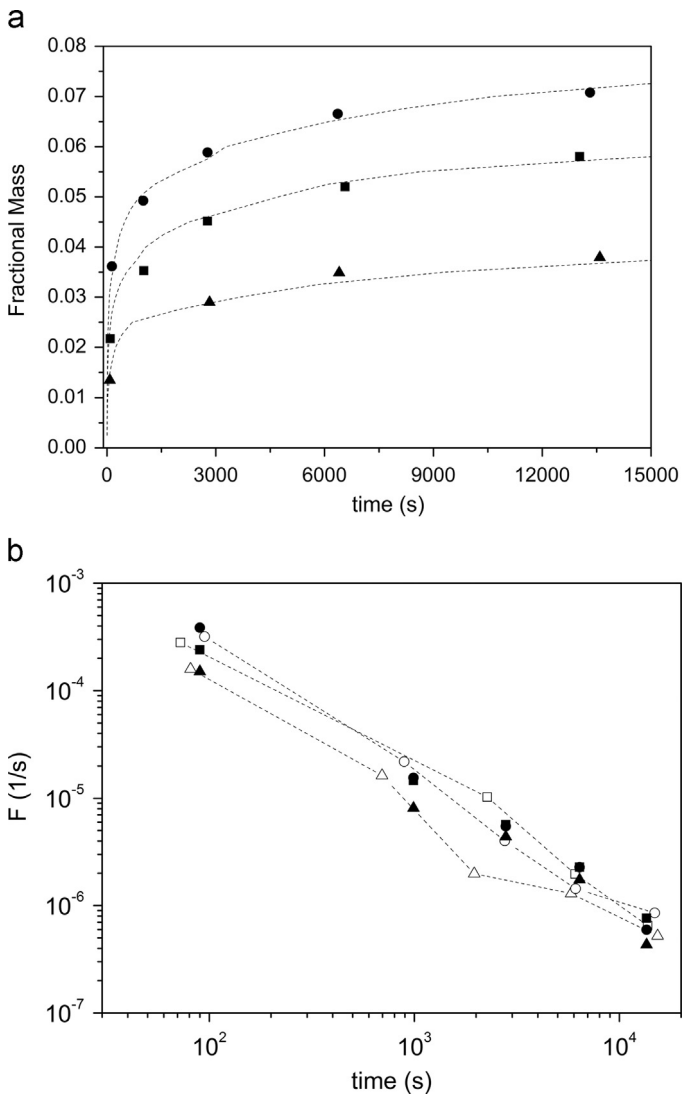

Fig. 10. (a) Comparison with experimental data from Giess et al. (1997). The symbols are the experimental results for the resuspended fractional mass vs. time and the dashed lines are the result of our simulations. From top to bottom, the curves correspond to wind speeds of 7.8, 5 and 3 m/s, respectively. The simulation parameters are $\mu_a = 37.0 \times 10^{-11}$ N, $\mu_b = 15.6 \times 10^{-13}$ N; $\mu_a = 14.7 \times 10^{-11}$ N, $\mu_b = 4.9 \times 10^{-13}$ N; $\mu_a = 3.75 \times 10^{-11}$ N, $\mu_b = 0.87 \times 10^{-13}$ N, respectively. (b) Resuspension rates for experiments and simulations. The filled symbols correspond to experimental data and the open symbols plus lines correspond to simulations.

central one is the LTS region. This diagram gives a rough idea of the resuspention behavior expected for a certain set of force parameters.

3.4. Comparison with experimental results

To test the predictive potential of the model, in this section we present some comparisons with experimental data from Giess et al. (1997) for a monolayer of particles. In their experiments, the authors measured the resuspension of particles from grass swards exposed to three wind speeds inside a wind tunnel. The particles used were monodisperse porous silica, and the fractional mass of material removed from the surface as a function of time is reported in the paper. It is worthy to say that we only seek to compare the simple process of particle resuspension in a steady state hydrodynamic flow and for a monolayer of particles in order to provide at least a minimum contrast of our model with experiments and to evidence its potential.

Results for three wind speeds (3 m/s, 5 m/s and 7.8 m/s) with 1 μm diameter particles, deposited on a short grass canopy, are chosen here to be compared with our model. The experimental results correspond to the fractional mass of resuspended particles vs. time. Thus, for the present calculation of our model, we set μ_b according to the size of the particles in the experiment, and the corresponding friction velocities (intervening through τ_m) reported by the authors: 0.27 m/s, 0.64 m/s

and 1.14 m/s, respectively. In the absence of any other experimental information, we keep the relation between the mean burst force and the dispersion as in most cases, i.e., we take $\sigma_b = 0.33\mu_b$. Given that experimental values for the fractional mass of removed material resulted to be very low for the three wind speeds (see Fig. 3 in Giess et al., 1997), the values for μ_a and σ_a are chosen accordingly to fall into an LT regime. To reduce the number of possible values for the adhesion parameters, we fix $\sigma_a = 2.0$, which is a reasonable value inside the LT region.

Figure 10(a) shows the results obtained for the three wind speeds. They are easily obtained from the simulations by direct counting of resuspended particles as time evolves, divided by the initial total mass. The resulting adhesion force and dispersion for each case are indicated in the legend. Each value reported there is only an estimation of the mean force and is quite close to the expected range reported in the literature for different systems (Ranade, 1987; Ripperger & Hein, 2005; Salazar-Banda et al., 2007) . The time scale corresponds to the same frequency factor, ν, used before. Figure 10(b) shows the simulation results for the resuspension rate calculated from the integral mass resuspension and compared with the corresponding rate values of Giess et al. (1997). The open symbols and lines represent the results from our simulation and the filled symbols to the experiments of Giess et al. (1997). Each symbol is in correspondence with those in part (a). The agreement found is good.

We observe that the aerodynamic forces are greater as the wind speed increases. Looking at the values found for the adhesion forces in each case, the results show that μ_a increases as the wind speed increases. This is in the sense of the discussion given by Giess et al. (1997), on the expected behavior for a surface such as grass, where the wind speed can influence the movement of the leaves and, consequently, the exposure of the particles to the wind flow. Thus, since the leaves are folded over, shielding aerodynamic effects, the apparent behavior is as if the adhesion force would increase as the wind speed is higher. Although this effect is only discussed in that paper for the comparison of behavior on long and short grass, we guess that this effect could be present in the case of short grass at different wind speeds. Nevertheless, we should say that our model is not able to distinguish (because of the independence between μ_a and μ_b) between the possible role that the leaf shielding may play in the aerodynamic forces or between the presence of a more intense adhesion force. For that reason, our explanation about the effect of the increase in μ_a as the wind speed increases is just a way of looking at an apparent effect.

We should say that the comparison presented in Fig. 10 is not precisely the result of a fit, but rather the direct search (without any minimization) for parameters that best represent the experimental behavior. It is worthy to say that a change in the value of ν would affect the obtained value for μ_a. As soon as a reliable value for ν could be obtained from experimental data, the obtained value for μ_a would be closer to reality. Taking this in mind, the agreement found is quite good. In this way, we are able to find the adhesive force distribution to be expected for a particular experimental setup.

4. Discussion

The results for the simulation of a surface with a monodisperse set of adhesion forces are in agreement with the expected behavior reported in the literature. The discussion becomes more interesting when roughness is present and, in that scenario, we are able to distinguish three different shapes for the curves of resuspension flux vs. time: one corresponding to a short time resuspension and two corresponding to a long time resuspension regime.

4.1. Parameters influencing the resuspension behavior

The particular shape for the flux in a given reentrainment process will depend on the parameters, defining the strength and dispersion of the forces participating in it. From the whole set of simulations performed here (partly shown in Table 1) we could say that it is necessary to know, at least, the difference between the mean values of forces, $\Delta\mu$, and the dispersion of adhesion forces, σ_a, to predict the time extent of the resuspension process. For example, we do not find a case of long-time resuspension (without a shoulder) and $\Delta\mu > 0$ (see Table 1 and Fig. 8).

For the particular case of long time resuspension with a shoulder (see for example Fig. 4), we note a large flux value at the beginning (as in the case of a short time process) but, after a few seconds, it rapidly decays several orders of magnitude to achieve a $1/t$ behavior for long times. It is for this reason that we speak here of some sort of change in behavior, from a short time to a long time resuspension regime. This happens, for instance, in a system where $\Delta\mu$ is small (favoring shorter times) but the dispersion of adhesion forces is very large (favoring longer times). This is clearly seen when comparing case 2 with case 5, or case 9 with 11, in Table 1. When resuspension exhausts those particles adhered with forces close in magnitude to a typical burst, the process is then delayed since particles still resting on the surface are strongly adhered to it. This behavior is in agreement with the knowledge that for sufficiently wide initial adhesion force distributions, flow decays inversely proportional to time (Reeks et al., 1988; Wen & Kasper, 1989).

It is important to discuss the long-term behavior found in our simulations. In Table 1, we report the slopes arising from a linear fit performed on the last points of the resuspension curve. For the case of short time resuspension, the values range from 1.35 to 4.1, far, in general, from a $1/t$ behavior. It is important to note that the short time resuspension behavior was never observed for values of σ_a larger than 1.5. This reinforces the discussion above. For cases with long-term resuspension tail, the slopes are between 1.16 to 1.01, in close agreement with the results for other models and the expected $1/t$ behavior (Reeks et al., 1988; Nicholson, 1993).

Concerning the parameters included in the phase-diagram, it is important to note the relative effect of Ω on the shape of the curves. For example, case 3, which belongs to the LT region, has a value of Ω close to the one for other cases presenting a shoulder (as in 5, 8, 11 or 23). In this scenario, it is important to see that $\Delta\mu$ is positive for these last cases compared with its negative value for case 3. Besides, care must be taken when analyzing the correlation between σ_a and Ω, since if we fix the aerodynamic force distribution, the fact that σ_a increases does not mean that Ω increases. This is due to the particular shape of the log-normal distribution (for example, compare cases 1 and 4).

4.2. Comparison with other models and experiments and possible extensions

Comparing the results here with the behavior reported by other models and experiments, we find that they qualitatively span quite well the resuspension curves reported elsewhere (Reeks et al., 1988; Wen & Kasper, 1989; Giess et al., 1997; Friess & Yadigaroglu, 2001, 2002). Furthermore, looking at the results for the resuspension flux vs. time reported by Friess & Yadigaroglu (2002) (see Fig. 3 in that paper) we see that the curves can be qualitatively described by our MC simulations, provided that a good set of parameters for adhesion and aerodynamic forces is chosen (see Fig. 3 here). Indeed, as the general qualitative behavior is quite good when the case of a single monolayer is compared, and taking into account that the behavior is qualitatively similar to the multilayer case, we believe that a particle–particle interaction or a modification of the adhesion forces could be incorporated without difficulty in our model to simulate an effective cluster adhesion.

In particular, the comparison with the experimental results of Giess et al. (1997) is quite good. We find that adhesion forces increase as soon as the wind speed increases in the tunnel. We relate this finding to the screening of the particles from the wind bursts. However, as pointed out above, another interpretation may be put forward concerning the role that leaf shielding may have on the aerodynamic forces during a resuspension process like the one in the experiments.

The results of this comparison open the possibility to find the parameters for the adhesion force distribution, given those corresponding to the aerodynamic force distribution and the curve of resuspended mass vs. time. Besides, it is important to remark that the values of the adhesion forces predicted by the model will become more accurate as soon as the value of the frequency ν will be fully characterized by experimental data.

The possibility to account for the ratio between adhesion and hydrodynamic moments, as in the Rock'n'Roll model from Reeks & Hall (2001), or even the energy ratio between external excitation and bounding potentials, is also straightforward, as it will be concluded in the next section. On the other hand, and concerning the possibility of extending our model to include the idea of treating turbulence fluctuations as impulses (Celik et al., 2010; Valyrakis et al., 2011), we believe that the present model could be used for that purpose with appropriate changes, but not in its present form.

The advantage of using a Metropolis algorithm in the context of the MC method presented here is that no integrals have to be done in order to calculate the resuspension probability for particles. This turns our model in a versatile tool to simulate a reentrainment process.

5. Conclusion

The model presented in this paper is based on simple and well known simulation methods, commonly used in the adsorption–desorption problem on surfaces. It proves to adequately span all the possible features for particle resuspension flux.

Our results show that short-term resuspension is related to Ω and to part of adhesion force distribution being lower than the smallest aerodynamic force, while the long-term resuspension is linked also to Ω and part of adhesion force distribution remaining above the highest aerodynamic force, thus, the change in behavior is expected to depend on both, dispersions in adhesion and aerodynamic forces.

The phase-diagrams presented in Figs. 8 and 9, demonstrate that three different regions of behavior can be isolated and characterized by a certain range of values for three parameters: $\Delta\mu$, σ_a and Ω. These diagrams are a rough guide to predict the expected behavior when the force parameters present in the problem are given.

The comparison with experimental data proves the prediction capability of the model, setting the challenge for future work, especially for the case of other force distribution shapes.

In the statement of Eq. (5), one might have chosen an energy ratio instead of the force ratio. If the data of the interaction potentials between the particles and the surface, or between the particles and the turbulent flow is provided, this implementation can be done very easily in our model. Moreover, in the same Eq. (5), one can choose a moment balance as the exponent defining the resuspension rate. In that case, care should be taken to redefine the meaning of each of the forces participating in the statement.

The temporal scale could be tuned to experimental results by an appropriate choice of the frequency in Eq. (5), this choice should be related to the burst occurrence frequency.

Finally, this model complements the interesting and important contributions of previous models (Zhang, 2011), incorporating here the stochastic nature of the complex process of resuspension and the interaction forces that appear in it.

On the other hand, our model presents the advantage of being versatile (any distribution for the forces can be used) with parameters that are clearly identified with the forces intervening in the problem, and can easily be converted into physical input parameters provided by experimental data. The simulation time elapsed in each run is reasonable and we do not have to solve any integral equation.

Acknowledgments

This work was supported by CONICET (Argentina) through Grant PIP no. 1022 and by the Secretary of Science and Technology of Universidad Nacional de San Luis, Grant P-3-1-0114. The authors want to thank Dr. Octavio Furlong (UNSL) for his contribution to this paper.

References

Binder, K., & Heermann, D.W. (1992). *Monte Carlo Simulation in Statistical Physics: An Introduction* 2nd ed.). Springer Verlag: Berlin.
Bohme, G., Krupp, H., Rabenhorst, H., & Sandstede, G. (1962). Adhesion measurements involving small particles. *Transactions of the Institution of Chemical Engineers*, *40*, 252–259.
Boor, B.E., Siegel, J.A., & Novoselac, A. (2013). Monolayer and multilayer particle deposits on hard surfaces: literature review and implications for particle resuspension in the indoor environment. *Aerosol Science and Technology*, *47*, 831–847.
Bowling, R.A. (1988). *A Theoretical Review of Particle Adhesion. Particles on Surfaces I: Detection, Adhesion and Removal* (pp. 129–142)Plenum Press: New York 129–142.
Celik, A.O., Diplas, P., Dancey, C.L., & Valyrakis, M. (2010). Impulse and particle dislodgement under turbulent flow conditions. *Physics of Fluids*, *22*, 046601.
Csavina, J., Field, J., Taylor, M.P., Gao, S., Landázuri, A., Betterton, E.A., & Sáez, A. (2012). A review on the importance of metals and metalloids in atmospheric dust and aerosol from mining operations. *Science of the Total Environment*, *433*, 58–73.
Friess, H., & Yadigaroglu, G. (2001). A generic model for the resuspension of multilayer aerosol deposits by turbulent flow. *Nuclear Science and Engineering*, *138*, 161–176.
Friess, H., & Yadigaroglu, G. (2002). Modelling of the resuspension of particle clusters from multilayer aerosol deposits with variable porosity. *Journal of Aerosol Science*, *33*, 883–906.
Fu, S.C, Chao, C.Y.H, So, R.M.C., & Leung, W.T. (2013). Particle resuspension in a wall-bounded turbulent flow. *Journal of Fluids Engineering*, *135*, 041301.
Giess, P., Goddard, A.J.H., & Shaw, G. (1997). Factors affecting particle resuspension from grass swards. *Journal of Aerosol Science*, *28*, 1331–1349.
Goldasteh, I., Goodarz, A., & Ferro, A.R. (2013). Monte Carlo simulation of micron size spherical particle removal and resuspension from substrate under fluid flows. *Journal of Aerosol Science*, *66*, 62–71.
Gradón, L. (2009). Resuspension of particles from surfaces: technological, environmental and pharmaceutical aspects. *Advances in Powder Technology*, *29*, 17–28.
Guingo, M., & Minier, J.-P. (2008). A new model for the simulation of particle resuspension by turbulent flows based on a stochastic description of wall roughness and adhesion forces. *Journal of Aerosol Science*, *39*, 957–973.
Hanus, M.J., & Langrish, T.A.G. (2007). Resuspension of wall deposits in spray dryers. *Journal of Zhejiang University Science A*, *8*(11), 1762–1774.
Henry, C., Minier, J.-P., & Lefreve, G. (2012). Numerical study on the adhesion and reentrainment of nondeformable particles on surfaces: the role of surface roughness and electrostatic forces. *Langmuir*, *28*, 438–452.
Henry, C., & Minier, J.-P. (2014a). Progress in particle resuspension from rough surfaces by turbulent flows. *Progress in Energy and Combustion Science*, *45*, 1–53.
Henry, C., & Minier, J.-P. (2014b). A stochastic approach for the simulation of particle resuspension from rough substrates: model and numerical implementation. *Journal of Aerosol Science*, *77*, 168–192.
Ibrahim, A.H., Dunn, P.F., & Qazi, M.F. (2008). Experiments and validation of a model for microparticle detachment from a surface by turbulent air flow. *Journal of Aerosol Science*, *39*, 645–656.
Matsusaka, S., Aoyagi, T., & Masuda, H. (1991). Unsteady particle-reentrainment model based on the internal adhesive strength distribution of a fine powder layer. *Kagaku Kogaku Ronbunshu*, *17*, 1194–1200.
Meng, B., & Weinberg, W.H. (1994). Monte Carlo simulations of temperature programmed desorption spectra. *Journal of Chemical Physics*, *100*, 5280–5289.
Metropolis, N., Rosenbluth, A.W., Rosenbluth, M.N, Teller, A.H., & Teller, E. (1953). Equation state calculations by fast computing machines. *Journal of Chemical Physics*, *21*, 1087–1092.
Moelwyn Hughes, E.A. (1971). *The Chemical Statics and Kinetics of Solutions*. Academic Press: London.
Nicholson, K.W. (1993). Wind tunnel experiments on the resuspension of particulate material. *Atmospheric Environment*, *27A*, 181–188.
Ranade, M.B. (1987). Adhesion and removal of fine particles on surfaces. *Aerosol Science and Technology*, *7*, 161–176.
Reeks, M.W., Reed, J., & Hall, D. (1988). On the resuspension of small particles by a turbulent flow. *Journal of Physics D: Applied Physics*, *21*, 574–589.
Reeks, M.W., & Hall, D. (2001). Kinetic models for particle resuspension in turbulent flows: theory and measurement. *Journal of Aerosol Science*, *32*, 1–31.
Ripperger, S., & Hein, K. (2005). Measurement of adhesion forces in air with the vibration method. *China Particuology*, *3*, 3–9.
Salazar-Banda, G.R., Felicetti, M.A., Gonçalves, J.A.S., Coury, J.R., & Aguiar, M.L. (2007). Determination of the adhesion force between particles and a flat surface, using the centrifuge technique. *Powder Technology*, *173*, 107–117.
Sales, J.L., Uñac, R.O., Gargiulo, M.V., Bustos, V., & Zgrablich, G. (1996). Monte Carlo simulation of temperature programmed desorption spectra: a guide through the forest for monomolecular adsorption on a square lattice. *Langmuir*, *12*, 95–100.
Sales, J.L., & Zgrablich, G. (1987). Thermal desorption of interacting molecules from heterogeneous surfaces. *Physical Review B*, *35*, 9520–9528.
Sitja, G., Uñac, R.O., & Henry, C.R. (2010). Kinetic Monte Carlo simulation of the growth of metal clusters on regular array of defects on insulator. *Surface Science*, *604*, 404–408.
Stempniewicz, M.M., Komen, E.M.J., & deWith, A. (2008). Model of particle resuspension in turbulent flows. *Nuclear Engineering and Design*, *238*, 2943–2959.
Stovern, M., Felix, O., Csavina, J., Rine, K.P., Russell, MacK R., Jones, R.M., King, M., Betterton, E.A., & Sáez, A.E. (2014). Simulation of windblown dust transport from a mine tailings impoundment using a computational fluid dynamics model. *Aeolian Research*, *14*, 75. http://dx.doi.org/10.1016/j.aeolia.2014.02.008.
Taheri, M., & Bragg, G.M. (1992). A study of particle resuspension in a turbulent flow using a preston tube. *Aerosol Science and Technology*, *16*, 15–20.
Valyrakis, M., Diplas, P., & Dancey, C.L. (2011). Entrainment of coarse grains in turbulent flows: an extreme value theory approach. *Water Resources Research*, *47*, W09512.
Wen, H.Y., & Kasper, G. (1989). On the kinetics of particle reentrainment from surfaces. *Journal of Aerosol Science*, *20*, 483–498.
Zhang, F. (2011). *The Modelling of Particle Resuspension in a Turbulent Boundary Layer* (Ph.D. thesis). School of Mechanical and System Engineering Newcastle University: (United Kingdom, and Laboratoire de Mécanique des Fluides et d'Acoustique Ecole Centrale de Lyon, France, and references there in).
Zhang, F., Reeks, M., & Kissane, M. (2013). Particle resuspension in turbulent boundary layers and the influence of non-Gaussian removal forces. *Journal of Aerosol Science*, *58*, 103–128.
Zhdanov, V.P. (1991). *Elementary Physicochemical Processes on Solid Surface*. Plenum Press: New York, London.
Ziskind, G., Fichman, M., & Gutfinger, C. (1995). Resuspension of particles from surfaces to turbulent flows—review and analysis. *Journal of Aerosol Science*, *26*, 613–644.
Ziskind, G. (2006). Particle resuspension from surfaces: revisited and re-evaluated. *Reviews in Chemical Engineering*, *22*, 1–110.
Zhou, H., Götzinger, M., & Peukert, W. (2003). The influence of particle charge and roughness on particle–substrate adhesion. *Powder Technology*, *135–136*, 82–91.